A Parametric Study on the Inception and Evolution of Underground Coal Fires Based on a Lab-Scale Experimental Setup

Jun Li (iD) *, Key Laboratory of Efficient Utilization of Low and Medium Grade Energy, Ministry of Education, Tianjin University, Tianjin 300350, China and State Key Laboratory of Coal Resources and Safe Mining, China University of Mining and Technology, Xuzhou 221116 Jiangsu Province, China*

Pengbin Fu, Key Laboratory of Efficient Utilization of Low and Medium Grade Energy, Ministry of Education, Tianjin University, Tianjin 300350, China

Yandong Mao, State Key Laboratory of Coal-Based Low Carbon Energy, Enn Technology and Development Co. Ltd., Langfang 065001 Hebei Province, China

Varinder Saini, Department of Civil Engineering, Indian Institute of Technology Ropar, Rupnagar, Punjab 140001, India

Ellina Sokol, Institute of Mineralogy and Petrography, United Institute of Geology, Geophysics and Mineralogy, Siberian Branch of the Russian Academy of Sciences, Novosibirsk, Russia 630090

Abstract. The tendency of self-ignition of coal is the root cause of underground coal fires (UCFs). A parametric study is carried out on a lab-scale experimental setup developed based on the essential heat and mass transfer characteristics of actual UCFs to understand the factors influencing the inception and evolution of coal fires. Effects of heat accumulation, moisture content and coal layer height are systematically examined by varying the relevant parameters on the experimental setup. Temporal evolution of coal temperature and volumetric fractions of CO and CO_2 are measured and analyzed. The results indicate that heat accumulation, moisture content and coal layer height mainly influence the time needed to reach the ignition state. Without sufficient heat accumulation, coal–oxygen reactions are not self-sustainable even after they enter the rapid reaction stage. The reaction regimes inside the coal tank are mainly determined by the local oxygen concentration, while the temperature changing rate depends on the relative magnitudes of heat generation and heat transfer (gain/loss). The ratio of CO_2/CO is more informative in the detection of high-temperature stage of UCFs.

---

* Correspondence should be addressed to: Jun Li, E-mail: lijun79@tju.edu.cn

1. Introduction

Underground coal fires (UCFs), a common disaster encountered in most coal-producing countries like China, the United States, Australia, India and many others, seriously threatens energy resources and mining safety and harms the environment and human health in the neighboring regions [1–4]. Early detection, effective control and extinguishment of UCFs are, therefore, of great social, economic and environmental significances at both regional and global scales.

UCFs are basically a result of continuous heat accumulation from coal–oxygen physio-chemical reactions. Besides UCFs, the tendency of coal self-ignition may also lead to spontaneous combustion of coal stockpiles [5–7]. The occurrence of UCFs is influenced by numerous factors such as the geophysical conditions of the overburden (formations, pores, fractures, fissures and permeability), the direction and depth of the coal seam(s), coal properties, the ambient temperature and humidity, solar irradiation, precipitation and many others. Besides coal properties, oxygen transport and heat accumulation are the two most important factors that directly influence the self-ignition of coal and subsequent fire evolution. Previous studies could be basically categorized into two groups. The first one focuses on coal–oxygen reactions [8–17] under well-controlled conditions with given oxygen concentrations, air flow rates and/or reactor temperatures. Forced air flows are guided to pass through isothermal [8–13] or adiabatic [14–17] reactors filled with coal particles to identify the reaction pathways and characteristic gaseous products. The second group takes into account the interaction of the coal seam(s) with neighboring elements (roof and bottom rocks, fractures, etc.) through coupled physical models [18–25], mainly used to understand the process of fire evolution.

The first group of studies employs forced air flows instead of natural convection which is a limiting factor to the reaction rates, while the second group of studies only deals with the high-temperature flame evolution. As such, both of them deviate from the actual conditions of most UCFs. In our early publication [26], a lab-scale experimental setup which includes the overburden to account for the seepage flows of air and exhaust gases with the natural convection as the only driving force was developed. By varying the fracture shape and dimensions as well as the thickness of the overburden, some preliminary results on the temporal variation of coal temperature, exhaust gases temperature and CO and CO_2 volumetric fractions were obtained [26]. The present study is meant to further investigate the effects of three key factors, they are, the heating pattern, the moisture content and the coal layer height, on the inception and evolution of underground coal fires by a parametric study, and to derive some rules applicable to the detection and prevention of actual UCFs. It needs to be pointed out that factors studied in Ref. [26] mainly influence the transport of oxygen and gaseous products of combustion, while the focus of the present study is on the heat transfer aspects. Besides the presentation of the experimental results, a simple theoretical model is also given at the end of this paper to analyze the heat transfer in the coal layer.

2. Experiment

The lab-scale experimental setup is schematically shown in Fig. 1 with some adaption to the figure in Ref. [26]. The most distinctive design feature of the setup is represented by the alumina (porous) foam placed on top of the coal layer—it is used to simulate the overburden with both fractures and pores, thus enabling seepage flows of air and gaseous products of combustion. The porosity of the alumina foam is about 0.8 to 0.9 and its thermal diffusivity is about 9.5×10^{-6} m^2/K. The stainless steel reaction tank has the dimensions of 200 mm (L), 200 mm (W) and 350 mm (H), with thermal insulation applied on the side and bottom walls to minimize heat losses to the ambient. An electric plate heater (square shape with the side length of 195 mm) is employed at the bottom of the coal layer in order to accelerate the ignition process. A constant electric power is applied to the heater, and therefore the boundary condition is an inert wall with a constant heat flux. K-type thermocouple probes are used to monitor the temperature within the coal layer. A gas sensor is anchored at the exit of the fracture to measure the volumetric fractions of CO and CO_2 of the gaseous products during the process. The uncertainty of the thermocouple probe is smaller than 2.5°C when the temperature is below 1300°C. For the gas sensor, it has the accuracy of $\pm$ 10 ppm (0 to 199 ppm) and $\pm$ 5% (200 to 20,000 ppm) for CO and $\pm$ 0.3 vol% $\pm$ 1% of the reading for CO_2. To avoid unnecessary repetition, readers are directed to Ref. [26] for more details of the experimental setup.

A through-hole with a rectangular cross-section sized 100×10 mm^2 is fabricated at the center of the alumina foam. The overburden thickness, denoted as H_{ob} in Fig. 1, is fixed as 60 mm in our experiment. The lignite sample is obtained from Hami of Xinjiang Uygur Autonomous Region, China. Results of its proximate and elemental analyses are shown in Tables 1 and 2, indicating that it has a
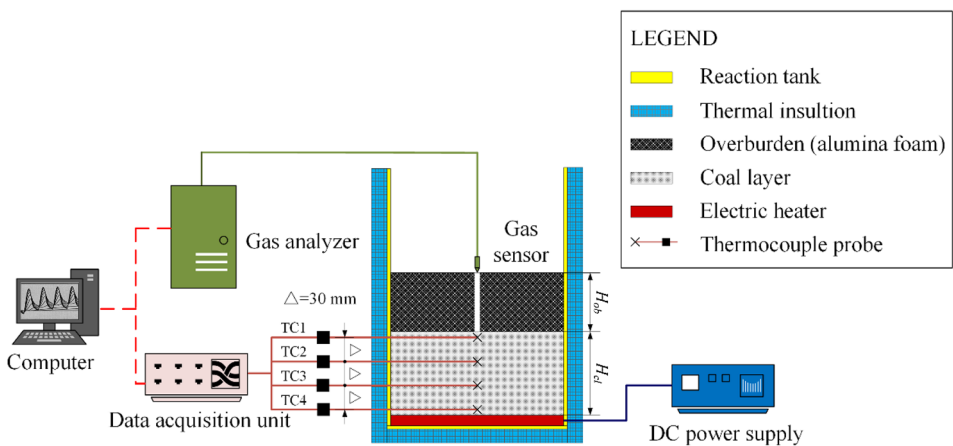

Figure 1. **Schematic of the experimental setup, adapted from Ref. [26].**

Table 1
Proximate analysis of coal sample

Moisture, M_{ar} (%)	Moisture, M_{ad} (%)	Ash, A_d (%)	Volatile matter, V_d (%)	Fixed carbon, FC_{ad} (%)	Heat content (dry fuel) (MJ/kg)	
					Gross calorific value	Net calorific value
23.82	12.71	11.57	43.27	32.45	26.084	25.067

Table 2
Elemental analysis of coal sample

Carbon, C_d (%)	Hydrogen, H_d (%)	Nitrogen, N_d (%)	Sulfur, S_d (%)
65.39	4.94	0.82	1.18

very high content of volatiles (43.27%). The raw coal is crushed into particles and further refined with stainless steel meshes to obtain the 1 to 2 mm particles for the experiment. The coal layer is formed by depositing coal particles uniformly to a given height, designated as H_{cl} in Fig. 1, which is a variable in this study. Three values are used, they are, 40 mm, 70 mm and 100 mm, with two, three and four thermocouple probes employed with an equal spacing of 30 mm, respectively.

As is mentioned above, the focus of the present study is on the heat transfer aspects. Since only one coal type is used, we only consider the moisture content in the experiment. As to heat accumulation, its effect is examined by varying the heating pattern (heating power and duration) of the electric heater and employing different values of H_{cl}. In summary, there are totally seven experimental cases designed in the present study and their detailed settings are given in Table 3. For

Table 3
Settings of the experimental cases

Case no.	H_{cl} (mm)	Heating power (W)	Stop heating halfway	Drying coal sample
1[a]	70	100	No	No
2	70	80	No	No
3	70	100	Yes[b]	No
4	70	100	Yes[c]	No
5	70	100	No	Yes
6	40	100	No	No
7	100	100	No	No

[a]Reference case
[b]Stops when the temperature changing rate at TC1 approaches 10 K/h
[c]Stops when the temperature at TC1 approaches 350°C

the detailed experimental procedure, readers are directed to refer to Ref. [26]. A minor change is made to the normal procedure when studying Cases 3 and 4, that is, turning off the electric heater at the critical time points, which will be elaborated in Sect. 3.2.

3. Results and Discussion

Prior to the parametric study, a repeatability test is carried out for the Reference case (Case 1, see Table 3) and the result is shown in Fig. 2. Two independent trials with identical experimental conditions are carried out and temperatures at different locations in the coal layer are measured over time. It can be seen that the consistency between the two independent trials is fairly satisfactory. The insignificant discrepancy is more likely to be caused by the uneven distribution of coal particle sizes used in the experiment. Based on the result shown in Fig. 2, the repeatability of our experimental setup is confirmed. As such, for the rest cases listed in Table 3, the experiment is conducted only once.

3.1. *Reference Case*

Firstly, temperatures at three locations (TC1, TC2 and TC3) in the coal layer are measured over time, based on which the temperature changing rate, that is, the temporal derivative, is obtained, and the results are plotted in Fig. 3. Interestingly, temperatures at the three locations exhibit greatly different patterns. TC3, which is located nearest to the electric heater, experiences a very sharp rise upon the start of the experiment but the changing rate gradually drops over time, as can be seen
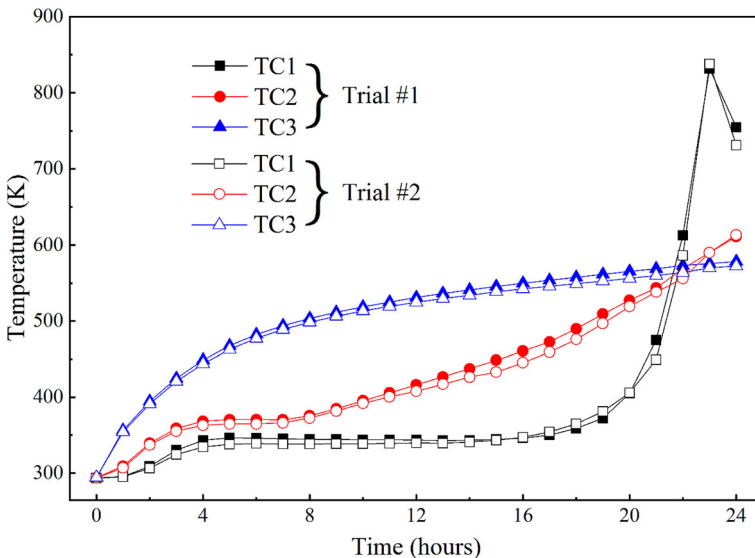

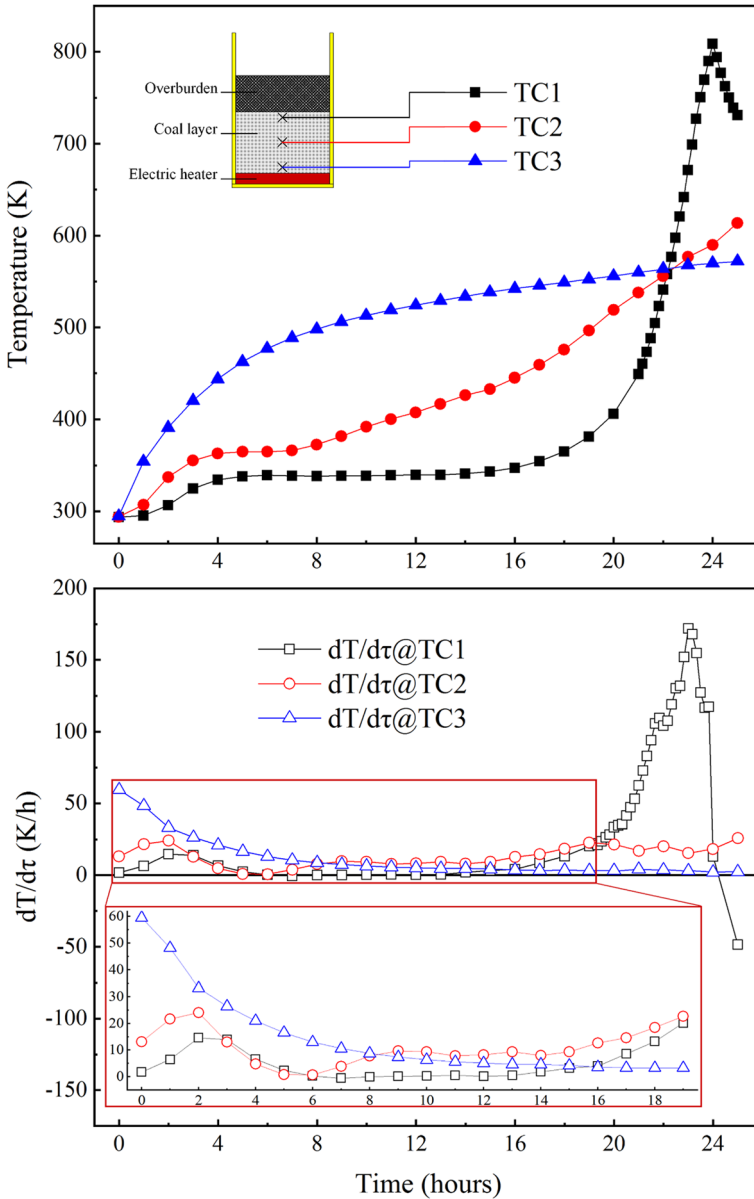**Figure 2.   Result of the repeatability test (Case 1).**

Figure 3. Temporal evolution of coal temperature and its changing rate (Case 1).

in Fig. 3. This is a clear indication that there are negligible chemical reactions but simply heat conduction from the bottom heater. Both TC2 and TC1 have a relatively 'flat' portion within which it is believed that endothermic reactions (mainly dehydration with some pyrolysis) dominate. For TC2, from the end of the 'flat'

portion, it enters a regime within which a nearly linear temperature increase is observed. In contrast, for TC1, its temperature history nearly follows an exponential pattern, with its magnitude quickly overtaking TC2 in about 6 h (from ~ 16 h to ~ 22 h). Based on the results shown in Fig. 3, it is believed that the two locations, TC1 and TC2, are actually controlled by different limiting factors that finally result in different reaction regimes, which will be elaborated with more details in Sect. 3.5.

Gaseous emissions from open vents or fractures in the field of UCFs are one of the most important features and are usually used as indicators for the existence of underground coal fires. Therefore, numerous studies have been carried out to identify the relationship between the coal–oxygen reaction temperature (reaction stage) and the corresponding gaseous emissions. Among the various gaseous products, CO and CO_2 are the two most commonly used index gases and their ratio is considered a very informative indicator. Wang et al. [10] found that the ratio of CO_2/CO closely depends on the coal temperature—it decreases with the increase of coal temperature, and the trend is more prominent below 70°C. Zhang et al. [15] studied a lignite coal in their experiment and obtained the ratio of CO_2/CO to be ~ 60 when the coal temperature is about 100°C, and its value drops to ~ 20 when the temperature reaches 200°C. Singh et al. [27] monitored the gaseous emissions in a coal fire field and their results indicate when the exhaust gases temperature is below 100°C, the volumetric fraction of CO_2 is usually 1–2 order of magnitude higher than that of CO. Wang et al. [28] experimentally examined CO_2 and CO formation during the low-temperature oxidation of a bituminous coal and noted that the ratio of CO_2/CO is ~ 3 when the coal temperature ranges between 60°C and 100°C. Similarly, Wu et al. [29] investigated the smouldering combustion of a bituminous coal and concluded that at the early-stage CO_2 is the primary product and its concentration is one order of magnitude higher than that of CO, with the ratio of CO_2/CO finally approaching ~ 3. For the purpose of comparison, the results of Refs. [10, 15, 28, 29] are compiled in Fig. 4. Apparently, coal properties have a profound impact on the ratio of CO_2/CO, and there exist remarkable discrepancies among various studies.

Take note that the above-mentioned results are obtained under well-controlled temperatures and oxygen concentrations that uniformly contain the coal sample. However, the uniform temperature and oxygen concentration within the coal layer cannot be achieved in our experiment, and it cannot happen in actual UCFs either. For both Case 1 and Case 2, the temporal evolution of volumetric fractions of CO_2 and CO measured at the exit of the fracture (see Fig. 1 for detailed placement position of the gas sensor) are obtained, based on which the ratio of CO_2/CO is quantified and plotted against the temperature at TC1 in Fig. 5. The relative magnitudes of both TC2 and TC3 are also included in Fig. 5. Because the measured CO and CO_2 fractions are actually a 'lumped' property—originating from various locations in the coal layer with different temperatures and different oxygen concentrations, therefore it does not reflect the condition of a localized point. Strictly speaking, the result obtained in our experiment is incomparable to those [10, 15, 28, 29] in the literature. Especially when the temperature at TC1 is below 350 K, our result in terms of the magnitude of CO_2/CO is abnormally high,
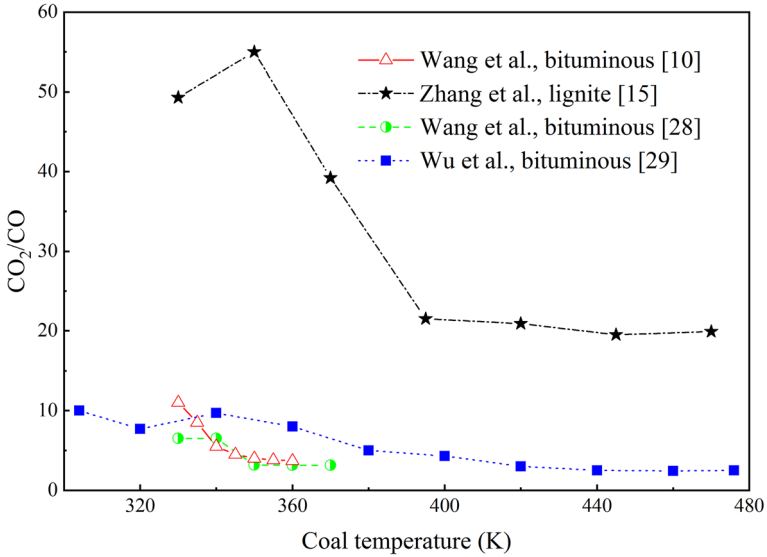
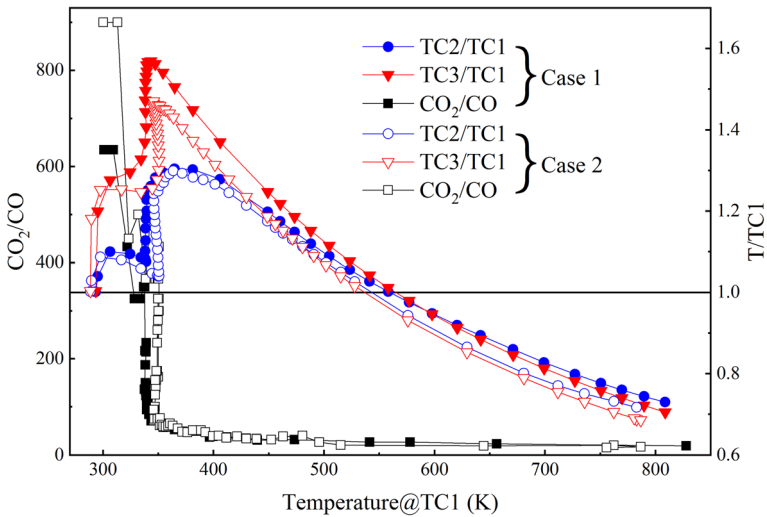**Figure 4. Literature review on CO_2/CO as a function of coal temperature.**

Figure 5. Temporal evolution of CO_2/CO with the coal temperature.

even higher than flaming combustion. A tentative explanation is that within that temperature range (< 350 K), very little CO is generated by pyrolysis, while the desorption of CO_2 from coal particles and the existence of CO_2 in the air (see the placement position of the gas sensor) together contribute to the high values of CO_2/CO. It is also indicated in Fig. 5 that when the temperature at TC1 is higher

than 350 K, the ratio of CO_2/CO gradually approaches a relatively stable value (~ 10). Based on the results obtained in our experiment and considering the actual conditions in UCFs, the applicability of the quantitative results reported in the literature to the detection of the low-temperature oxidation of coal in actual UCFs is very limited. Therefore, when conducting measurement in coal fields, it is proposed to continuously monitor the ratio over an extended period of time in order to obtain its variation trend to effectively judge the reaction stage.

3.2. Heating Pattern

By varying the power (Case 2) provided to the electric heater, the results on the temporal evolution of coal temperature and its changing rate are shown in Fig. 6. Since TC3 is basically a region with only heat conduction, its temperature changing rate is not included in Fig. 6. It can be seen that both Cases 1 and 2 successfully evolve to ignition and subsequently proceed to combustion. Although the time needed to enter the rapid reaction stage is longer for Case 2 (80 W), the peak temperatures and their changing rates at TC1 are almost identical for the two cases. This observation clearly indicates that when the oxygen concentration is sufficient, the peak combustion temperature is not much influenced by heat accumulation conditions. While at TC2, both temperature profiles are nearly linear with the slope (changing rate) of Case 2 is smaller than Case 1 (100 W).

To examine the self-sustainability of reactions upon turning off the electric heater, we first need to identify the critical time points. Zhao et al. [30] studied self-heating characteristics of an Indonesian lignite and noted that the rate of temperature rise is about 10 K/h when it enters the rapid reaction stage. As such, the first critical time point is chosen to be the moment when $dT/d\tau$ at TC1 is approaching 10 K/h, denoted as $\tau1$. Kok et al. [31] measured the ignition temperature of several lignite coals and found the value to be around 270°C–350°C. Therefore, the second critical time point is chosen to be moment when the coal temperature at TC1 approaches 350°C, denoted as $\tau2$. For Cases 3 and 4, the DC power supply is turned off at $\tau1$ and $\tau2$, respectively, and the results on the temporal evolution of coal temperature are shown in Fig. 7. For Case 3, the temperature at TC3 drops immediately after the electric heater is turned off, while the temperature at TC1 experiences a slight increase but shortly it starts to descend and no ignition takes place in the end, indicating that without sufficient heat accumulation, the oxidation reactions are not self-sustainable. Therefore, the implication of our result is that even though the coal temperature rise reaches the level of 10 K/h, it does not guarantee its ignition and further evolution to fires. In contrast, for Case 4, the temperature at TC1 continues to rise even after the electric heater is powered off, suggesting that once the coal is ignited the combustion is self-sustainable so long as there is sufficient oxygen (air) concentration. Having shown the above results, we can safely deduce that there exists a critical time point lying between $\tau1$ and $\tau2$—below that point the oxidation reactions are not self-sustainable. The identification of that critical point and its corresponding temperature could be of significant importance to the prevention and control of UCFs.
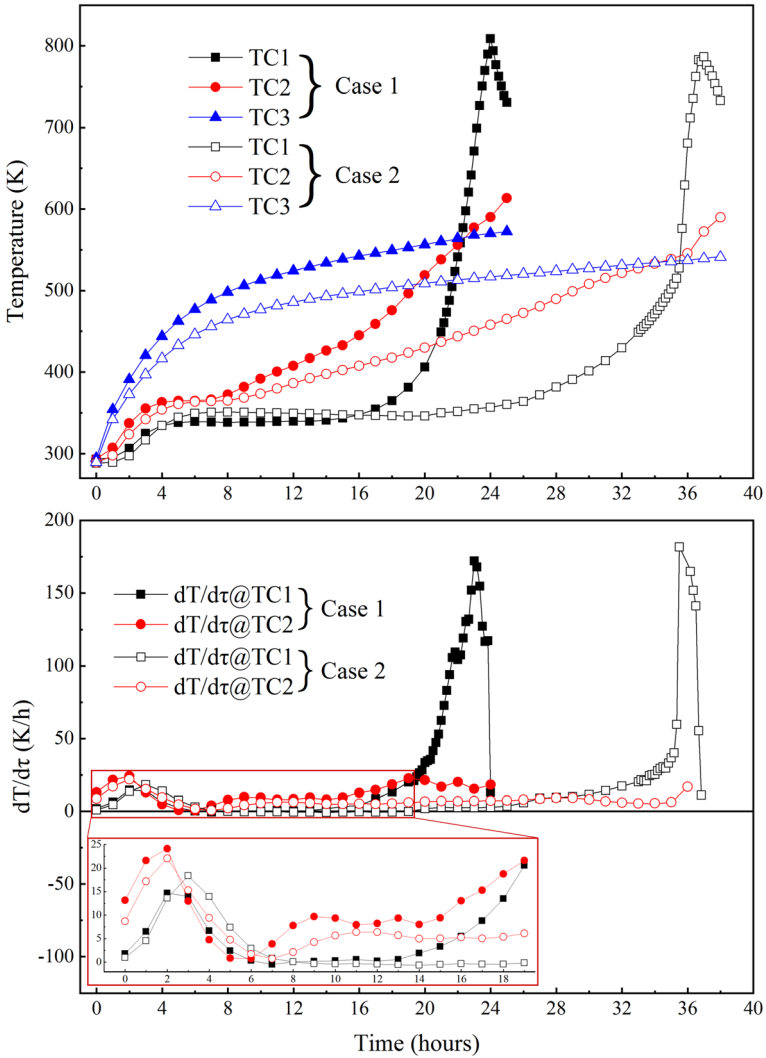
Figure 6. Effect of heating power on the temporal evolution of coal temperature and its changing rate.

3.3. Moisture Content

Moisture content in the coal is an important factor that influences the inception of UCFs. In order to examine the effect, the coal particles are dried in the vacuum oven at 40°C for 24 h. By measuring the mass loss, the moisture content upon drying is determined to be around 2.5%. The comparison of the temporal evolution of coal temperature between Case 1 and Case 5 is shown in Fig. 8. No sensible temperature difference exists at TC3, indicating that at TC3 there is essentially very little dehydration because the resistance of mass transfer (water vapor diffu-
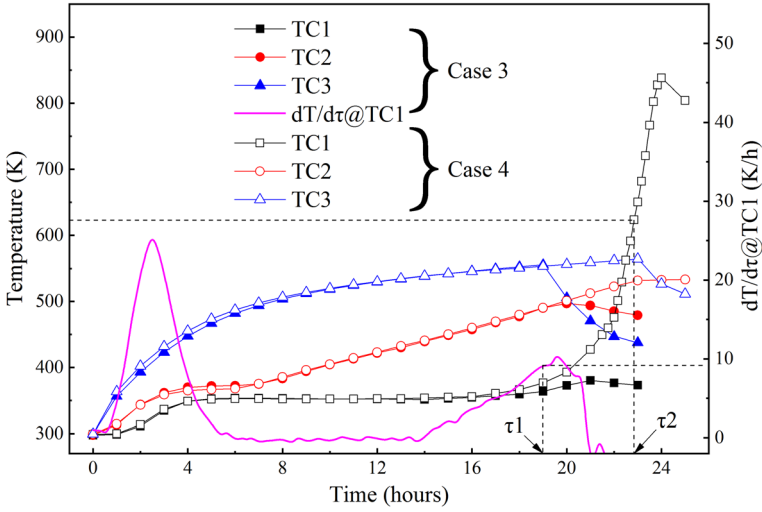
Figure 7. Effect of stopping heating at different time points on the temporal evolution of coal temperature.
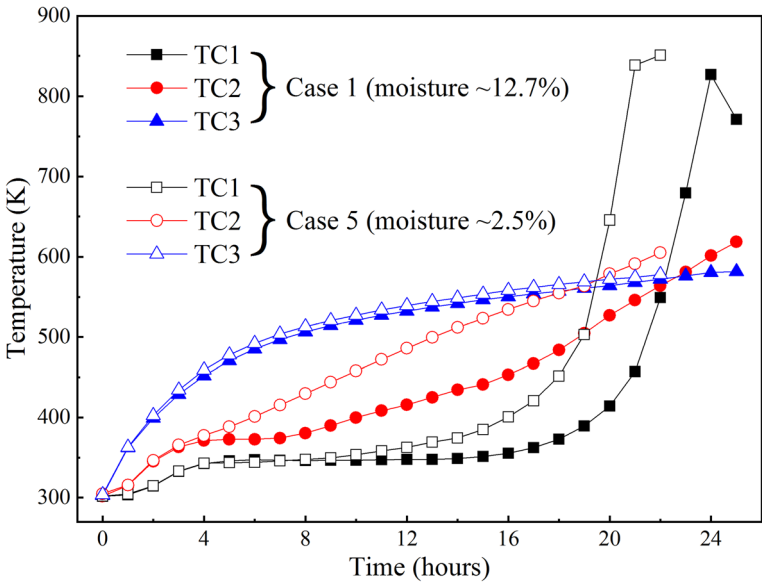

Figure 8. Effect of moisture content on the temporal evolution of coal temperature.

sion) is very high. For both TC2 and TC1, it can be seen that the length of the 'flat' portion is greatly reduced when the dried coal sample (Case 5) is used. However, it is found that in terms of the peak combustion temperature represented by TC1, the two coal samples exhibit almost identical values, implying that the mois-

ture content in the coal (seam) mainly influences the time needed to reach the inception of UCFs but does not affect the combustion temperature which depends more on the oxygen concentration. Therefore, coal seams with a lower moisture content are more prone to self-ignition under the same conditions of heat accumulation and oxygen (air) concentration.

Figure 9 further quantifies the temperature difference between the two moisture content cases for the three thermocouples. It can be seen that no significant difference occurs at TC3 where the mass transfer resistance is very high for the moisture vapor to diffuse out. The significant difference at TC1 is a result that the coal sample with a lower moisture content (Case 5) enters the rapid reaction stage much earlier than the one with a higher moisture content (Case 1).

3.4. Coal Layer Height (H_{cl})

In order to investigate the effect of coal layer height, two more values are employed, they are, 40 mm (Case 6) and 100 mm (Case 7), with two and four thermocouples to monitor the temperature in their coal layers, respectively. With the variation of the coal layer height, the packing density and the average porosity vary accordingly, with Table 4 showing the measurement results. The temporal evolution of coal temperature and its changing rate for Case 7 are illustrated in Fig. 10. Due to the scarcity of oxygen, temperature at both TC3 and TC4 exhibit a similar pattern of heat conduction, with a very short period of dehydration at TC3. With the increase of oxygen concentration in the upward direction, it can be seen that the temperature rise follows a linear trend at TC2 and an exponential trend at TC1, which is qualitatively similar to the Reference case (Case 1). Fur-
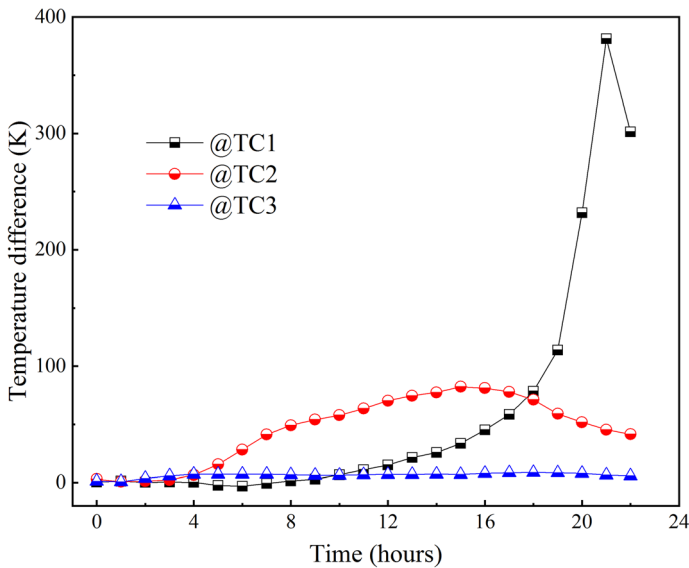

Figure 9.   Temperature difference at three thermocouples for different moisture concents (Case 1 and Case 5).

Table 4
Measured packing density and porosity for different H_{cl}

Coal layer height (mm)	Packing density (kg/m^3)	Porosity
40	0.876	0.270
70	0.886	0.262
100	0.894	0.256

thermore, the comparison of the temporal evolution of coal temperature at TC1 for the three cases are plotted in Fig. 11. Interestingly, the three temperature profiles exhibit a similar pattern except for the different lengths of the 'flat' portion, that is, the larger the coal layer height, the longer time needed to reach the self-ignition state. It is believed that the longer time could be attributed to two reasons. Firstly, less heat is conducted from the bottom heater for a larger coal layer height. Secondly, more moisture (vapor) generated at the lower portion diffuses upward and therefore it takes a longer time to get fully dehydrated at TC1. Upon entering the rapid reaction stage, no significant difference in terms of the peak combustion temperature among the three cases is observed in Fig. 11. However, an apparently higher value of $dT/d\tau$ is found for Case 1. At this moment of time, it is not very sure whether this is a truth or a so-called 'error'—the frequency of data collection is every 10 min, but it might be insufficient when the temperature changing rate is remarkably high. In other words, the actual $dT/d\tau$ depends on the frequency used and it might give 'erroneous' values if the frequency is not high enough. Higher data sampling frequencies will be used in our future work to confirm that observation.

3.5. Discussion

Essentially, the temperature and its changing rate inside the coal layer is a direct result of (heat and mass) transfer and physio-chemical reactions between coal and oxygen. Based on the measured temperature profiles of Cases 1–7, we have Fig. 12 depicting the reaction characteristics in the coal layer. Because no forced air flow is employed, the only channel for air diffusion is from the top, that is, the ambient. Hence, in the vertical direction the oxygen concentration decreases as it goes down, giving three reaction regimes, they are, kinetics-controlled, diffusion-controlled and heat conduction only, which is supported by the temperature profiles illustrated in the above-mentioned figures. Figure 12 also presents a 1D control volume based energy balance model. As no forced air flows are enabled, convective heat transfer is insignificant compared to conduction. Based on the 1D model, we can deduce that the temperature changing rate ($dT/d\tau$) is proportional to

$$\frac{\partial T}{\partial \tau} \propto \left(Q \cdot \dot{\omega} - \lambda \frac{\partial^2 T}{\partial x^2} \right) \tag{1}$$
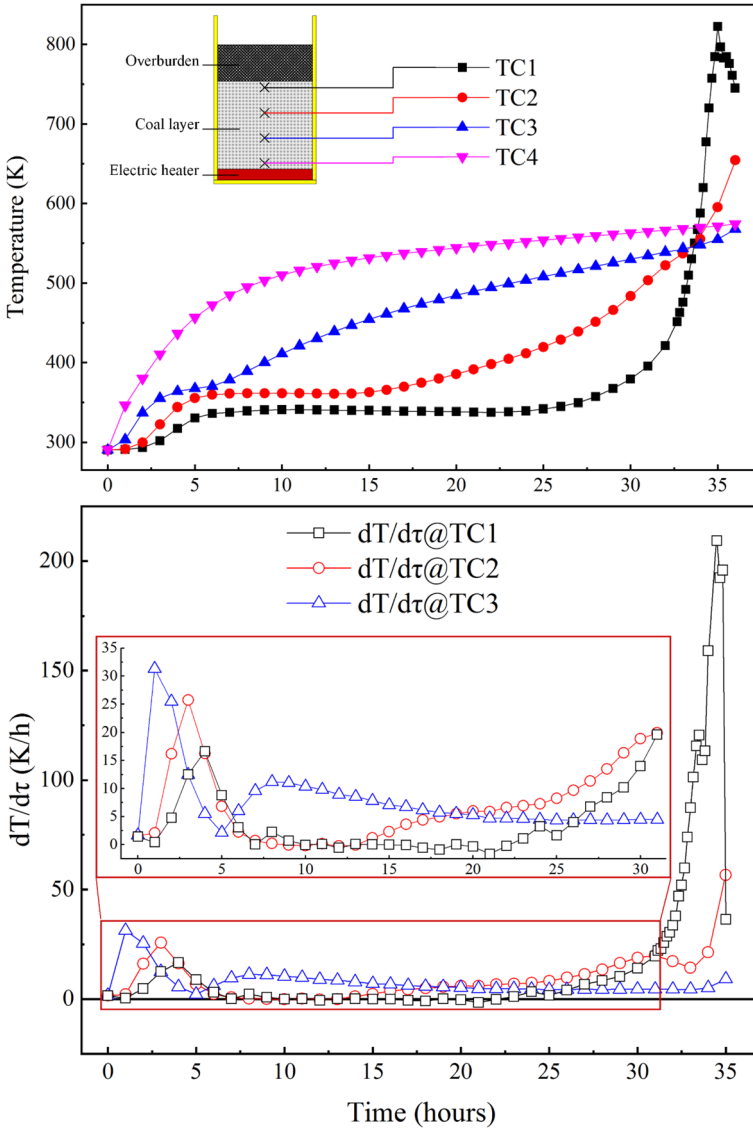
Figure 10. Temporal evolution of coal temperature and its changing rate (Case 7).

where Q is the caloric value of the specific coal sample (kJ/kmol), $\dot{\omega}$ the reaction rate (kmol/m^2 s) and λ the thermal conductivity of coal (W/m K). According to Arrhenius Law, the heterogeneous reaction rate of coal oxidation is governed by

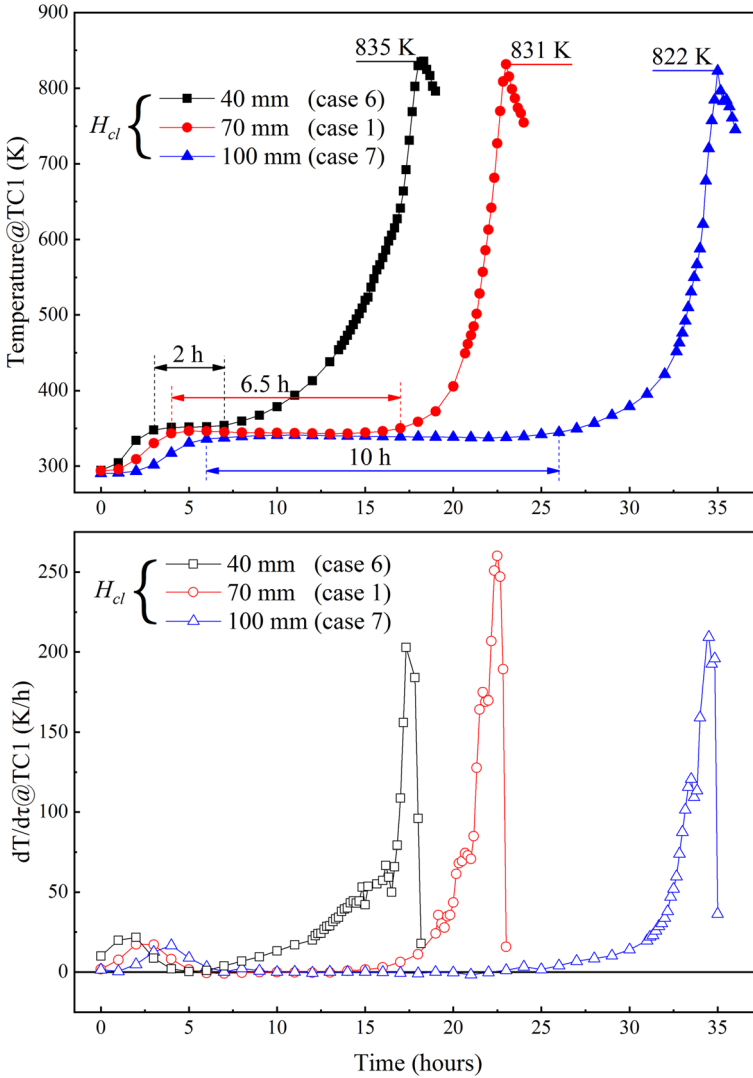$$\dot{\omega} = k_0 \exp\left(-\frac{E_A}{R_u T}\right)[O_2]^n \tag{2}$$

Figure 11. Effect of coal layer height on the temporal evolution of coal temperature and its changing rate at TC1.

where E_A is the activation energy, R_u the universal gas constant and n the reaction order. Figures 3 and 10 clearly show that the temperature profiles at TC1 exhibit an exponential pattern, indicating that the reaction regime is controlled by the local temperature. In contrast, the temperature profiles at TC2 follow a linear pattern, meaning that the reaction rate is mainly controlled by the diffusion rate of oxygen.
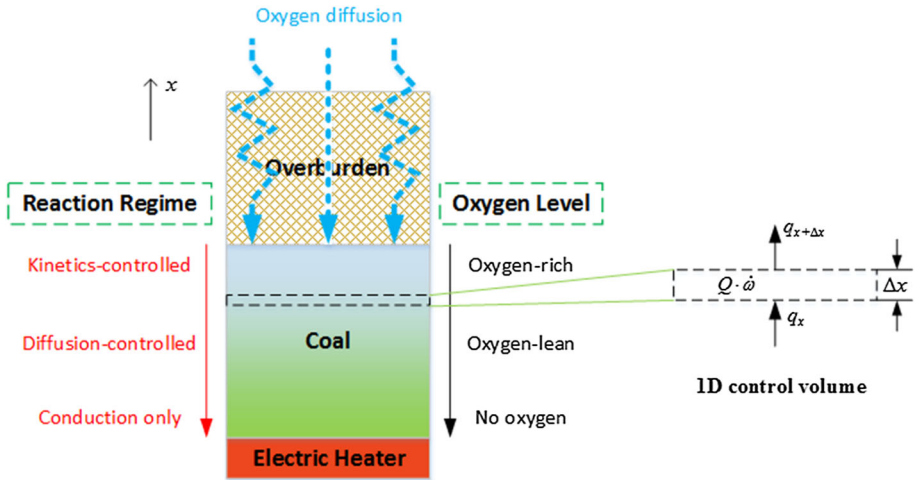
Figure 12. Schematic of reaction characteristics and 1D control volume in the coal layer.

To further illuminate the relative importance of the terms expressed in Eq. (1), three temperature values (450 K, 550 K and 650 K) are picked and the corresponding $dT/d\tau$ at those particular time points are acquired. Values at both TC1 and TC2 are compiled in Fig. 13 for the purpose of comparison. Within the duration of our experiment, the temperature at TC2 never reaches 650 K, and therefore Fig. 13 does not include $dT/d\tau$ at TC2 at 650 K. First of all, under the same temperature (450 K and 550 K), $dT/d\tau$ at TC1 gives a higher value than that at
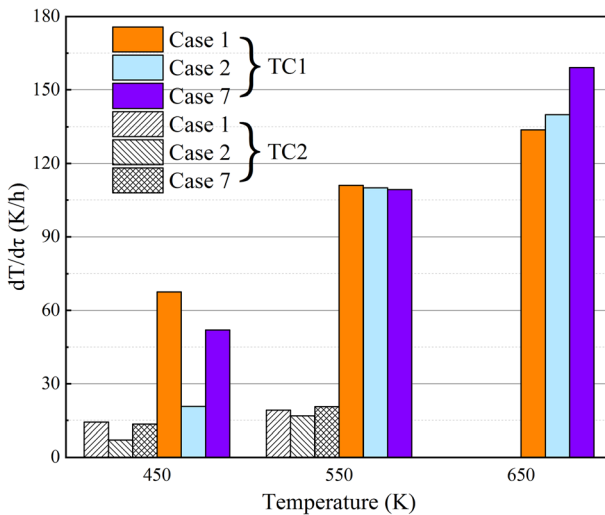

Figure 13. Comparison of coal temperature changing rates at different locations and coal temperatures.

TC2, manifesting the influence of oxygen concentration in Eq. (2). When $T = 550$ K, the difference among the three cases is very small, suggesting the second term (heat conduction) of the right-hand side of Eq. (1) is insignificant compared to the first term (heat generation). Thus, $dT/d\tau$ is simply a function of the local temperature and oxygen concentration. However, when $T = 450$ K, the term of heat conduction is not negligible anymore because Eq. (2) tells that $\dot{\omega}$ is proportional to $\exp(-1/T)$. When the coal temperature comes to $T = 650$ K, the term of heat conduction again becomes important because now at TC1 the temperature is very high and it transfers heat downwards via conduction. Under that condition, the larger coal layer height (100 mm) is more favorable in reducing heat loss to the lower part, and therefore represents a higher value of $dT/d\tau$ among the three cases. In summary, the temperature changing rate of a specific point in the coal layer is determined by both the local temperature and oxygen concentration but also the relative magnitudes of heat generation and heat transfer (gain or loss).

4. Conclusions

Based on the essential characteristics of heat and mass transfer in UCFs, a lab-scale experimental setup is built and a parametric study is undertaken to investigate the factors that influence the heat transfer aspects. The heating pattern, moisture content and coal layer height are examined systematically. Having analyzed the temporal evolution of coal temperature under different conditions, the main conclusions are made as follows:

1. Under the condition of sufficient oxygen concentration, heat accumulation only influences the time needed to reach the self-ignition state. Without sufficient heat accumulation, coal–oxygen reactions are not self-sustainable even after it enters the rapid reaction stage.
2. The effect of moisture content of coal sample simply lengthens the time needed to reach the self-ignition state.
3. With the increase of the coal layer height, it takes a longer time to reach the self-ignition state.
4. The temperature changing rate of coal is determined by both heat generation and heat transfer: the first term is governed by the local temperature and the oxygen concentration, while the second term by the relative magnitude of temperature.
5. Values of the ratio of CO_2/CO reported in the literature should be used with caution when they are compared with the results measured in actual coal fires, especially when judging the low-temperature stage of the coal–oxygen reactions.

Acknowledgements

References

1. Kuenzer C, Zhang J, Tetzlaff A et al (2007) Uncontrolled coal fires and their environmental impacts: investigating two arid mining regions in north-central China. Appl Geogr 27:42–62
2. Stracher GB, Taylor TP (2004) Coal fires burning out of control around the world: thermodynamic recipe for environmental catastrophe. Int J Coal Geol 59:7–17
3. Song Z, Kuenzer C (2014) Coal fires in China over the last decade: a comprehensive review. Int J Coal Geol 133:72–99
4. Melody SM, Johnston FH (2015) Coal mine fires and human health: What do we know?. Int J Coal Geol 152:1–14
5. Hooman K, Maas U (2014) Theoretical analysis of coal stockpile self-heating. Fire Saf J 67:107–112
6. Ejlali A, Mee DJ, Hooman K, Beamish BB (2011) Numerical modelling of the self-heating process of a wet porous medium. Int J Heat Mass Transf 54:5200–5206
7. Ejlali A, Hooman K (2011) Buoyancy effects on cooling a heat generating porous medium: coal stockpile. Transp Porous Media 88:235–248
8. Krishnaswamy S, Bhat S, Gunn RD et al (1996) Low-temperature oxidation of coal. 1. A single-particle reaction-diffusion model. Fuel 75:333–343
9. Beamish BB, Barakat MA, George JDS (2001) Spontaneous-combustion propensity of New Zealand coals under adiabatic conditions. Int J Coal Geol 45:217–224
10. Wang HH, Dlugogorski BZ, Kennedy EM (2003) Pathways for production of CO_2 and CO in low-temperature oxidation of coal. Energy Fuels 17:150–158
11. Fei Y, Aziz AA, Nasir S et al (2009) The spontaneous combustion behavior of some low rank coals and a range of dried products. Fuel 88:1650–1655
12. Yuan L, Smith AC (2011) CO and CO_2 emissions from spontaneous heating of coal under different ventilation rates. Int J Coal Geol 88:24–30
13. Deng J, Li QW, Xiao Y et al (2017) Experimental study on the thermal properties of coal during pyrolysis, oxidation, and re-oxidation. Appl Therm Eng 110:1137–1152
14. Qi G, Wang D, Zheng K et al (2015) Kinetics characteristics of coal low-temperature oxidation in oxygen-depleted air. J Loss Prev Process Ind 35:224–231
15. Zhang Y, Wang J, Wu J et al (2015) Modes and kinetics of CO_2 and CO production from low-temperature oxidation of coal. Int J Coal Geol 140:1–8
16. Wang DM, Xin HH, Qi XY et al (2016) Reaction pathway of coal oxidation at low temperatures: a model of cyclic chain reactions and kinetic characteristics. Combust Flame 163:447–460
17. Song Z, Huang X, Luo M et al (2017) Experimental study on the diffusion-kinetics interaction in heterogeneous reaction of coal. J Therm Anal Calorim 129:1625–1637
18. Rosema A, Guan H, Veld H (2001) Simulation of spontaneous combustion to study the causes of coal fires in the Rujigou Basin. Fuel 80:7–16

19. Wessling S, Kuenzer C, Kessels W et al (2008) Numerical modeling for analyzing thermal surface anomalies induced by underground coal fires. Int J Coal Geol 74:175–184
20. Wessling S, Kessels W, Schmidt M et al (2008) Investigating dynamic underground coal fires by means of numerical simulation. Geophysics Journal International 172:439–454
21. Huang J, Bruining J, Wolf K-H (2001) Modeling of gas flow and temperature fields in underground coal fires. Fire Saf J 2011(36):477–489
22. Liu W, Qin Y (2017) Multi-physics coupling model of coal spontaneous combustion in longwall gob area based on moving coordinates. Fuel 188:553–566
23. Wang Y, Shi G, Guo Z (2017) Heat transfer and thermodynamic processes in coal-bearing strata under the spontaneous combustion condition. Numerical Heat Transfer, Part A (Applications) 71:1–16
24. Wolf K-H, Bruining H (2007) Modelling the interaction between underground coal fires and their roof rocks. Fuel 86:2761–2777
25. Ide TS, Pollard D, Orr FM Jr (2010) Fissure formation and subsurface subsidence in a coalbed fire. Int J Rock Mech Min Sci 47:81–93
26. Li J, Fu PB, Zhu Q et al (2018) A lab-scale experiment on low-temperature coal oxidation in context of underground coal fires. Appl Therm Eng 141:333–338
27. Singh AK, Singh RVK, Singh MP et al (2007) Mine fire gas indices and their application to Indian underground coal mine fires. Int J Coal Geol 69:192–204
28. Wang HH, Dlugogorski BZ, Kennedy EM (2002) Examination of CO_2, CO, and H_2O formation during low-temperature oxidation of a bituminous coal. Energy Fuels 16:586–592
29. Wu DJ, Schmidt M, Huang XY et al (2017) Self-ignition and smoldering characteristics of coal dust accumulations in O_2/N_2, and O_2/CO_2 atmospheres. Proc Combust Inst 36:3195–3202
30. Zhao H, Yu J, Liu J et al (2015) Experimental study on the self-heating characteristics of Indonesian lignite during low temperature oxidation. Fuel 150:55–63
31. Kok MV, Pokol G, Keskin C et al (2004) Combustion characteristics of lignite and oil shale samples by thermal analysis techniques. J Therm Anal Calorim 76:247–254